Asian Journal of Chemistry; Vol. 27, No. 8 (2015), 3091-3096

ASIAN JOURNAL OF CHEMISTRY

http://dx.doi.org/10.14233/ajchem.2015.18907

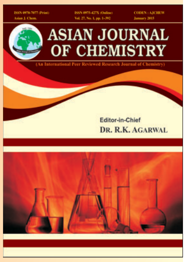

Theoretical and Computational Study of Tautomerization of Ketenimine to Acetonitrile

O.I. OSMAN[1,2,*]

[1]Chemistry Department, Faculty of Science, King Abdulaziz University, P.O. Box 80203, Jeddah 21589, Saudi Arabia
[2]Chemistry Department, Faculty of Science, University of Khartoum, P.O. Box 321, Khartoum 11111, Sudan

*Corresponding author: Fax :+966 6952109; Tel: +966 6952000 Ext. 69315; E-mail: oabdelkarim@kau.edu.sa

Received: 5 December 2014; *Accepted*: 2 January 2015; *Published online*: 27 April 2015; AJC-17199

ab initio electronic structure computations employing MP2, DFT(B3LYP) and CCSD methods with 6-311++G**, aug-cc-pvdz and aug-cc-pvtz basis sets have been performed for the equilibrium geometries and transition state involved in the interconversion between ketenimine (I) and acetonitrile (II). A direct unimolecular 1,3-hydrogen shift pathway for the ketenimine $\rightleftharpoons$ acetonitrile rearrangement was proposed. The activation energies of this mechanistic route range between 57.066 and 71.489 kcal/mol. They are in excellent agreement with the reported experimental value. The proposed tautomerization route was also supported by thermodynamic and natural bond orbital analyses.

Keywords: Ketenimine, Acetonitrile, Tautomerization, Activation energy, Hyperconjugation.

INTRODUCTION

Imines constitute a very important group of highly reactive compounds and they, therefore, caught the attention of many researchers[1-3]. As intermediates, they play an important role in the prebiotic synthesis of purines and proteins[4]. Their existence in space is extensively documented[5,6].

The first member of the imines series is methylenimine, CH_2=NH. It was as early as 1961 when methylenimine was detected, when methylazide was pyrolyzed in a solid argon and carbon dioxide matrix[7]. Subsequently, its microwave[8] and photoelectron[9] spectra were recorded. By 1973, its existence in dark interstellar clouds has been reported[10]. Methylenimine has also been subjected to extensive theoretical investigations[11-13] so as to explore its peculiar geometry and hence exceptional reactivity.

The next member in the imines series is ketenimine, CH_2=C=NH. It is a higher energy (32.03 kcal/mol) tautomer of acetonitrile, $CH_3C{\equiv}N$; but a lower energy (16.25 kcal/mol) tautomer of aminoacetylene, $HC{\equiv}CNH_2$[14]. Jacox and Milligan[15] observed the infrared spectrum of ketenimine when they reacted C_2H_2 and NH in solid argon. It took researchers more than twenty years to be able to observe gas phase ketenimine when Rodler *et al.*[16] managed to detect it by microwave spectroscopy in the pyrolysis products of 3-hydrosypropionitrile and 9.10-dihydro-9,10-(iminoethylene)anthracene. Later its photoelectron spectrum was reported by Kroto *et al.*[17]. The kinetics of the rearrangement of ketenimine to form acetonitrile is studied both experimentally and theoretically[18,19]. The thermal rearrangements on the C_2H_3N potential energy hypersurface has been studied theoretically by Lohr *et al.*[18]. Although they monitored the rearrangements of vinyl nitrene, 2H-azirine, methyl isocyanide and acetonitrile through a 1,2 hydrogen shift; they have not been able to locate a direct root leading to acetonitrile from ketenimine. Doughty *et al.*[19] using a shock waves experiment of a mixture of acetonitrile and argon at temperatures between 1400-1700 K and 12-15 atm pressure produced ketenimine with an activation energy of 70.251 ± 0.692 kcal/mol. The *ab initio* calculations accompanying this experiment predicted the ketenimine $\rightleftharpoons$ acetonitrile rate determining step to be the 1,2-hydrogen shift of the imine hydrogen producing vinyl nitrene.

In an experimental study we have been able to identify, among others, both prop-2-ynylideneamine and ketenimine, in the thermolysis products of iminodiacetonitrile in equimolar ratios[20]. As vinyl cyanide and acetonitrile were also present, which are tautomers of prop-2-ynylideneamine and ketenimine, respectively, we have conducted a thorough theoretical investigations of the two molecules and their tautomers and isomers. Our investigation of prop-2-ynylideneamine and its Z- and E-isomers together with its vinyl cyanide tautomer has been published elsewhere[21]. In this manuscript we strive to understand theoretically and computationally the manifestations of the tautomerization reaction of ketenimine and its tautomer acetonitrile through a 1,3-proton shift. Particularly, we contemplate to investigate the molecular structures and energies of these tautomers and their accompanying transition state. We plan also to support our molecular properties findings by natural bond orbital investigations. We believe that we can achieve these goals by computing: (1) the optimized geometries of these tautomers (2) the free energy changes and hence the equilibrium constants of the tautomerization reaction and (3) the hyperconjugation energies of the tautomers. These predictions have two functions: firstly, they allow comparisons to be made between the results obtained from the different theoretical levels and secondly, they shed light on the stabilities and reaction pathways of these tautomers.

COMPUTATIONAL DETAILS

All *ab initio* molecular orbitals calculations were performed using the Gaussian09 suite of programs[22]. The geometries of ketenimine, $CH_2=C=NH$ (I) and acetonitrile, $CH_3C\equiv N$ (II) were fully optimized to minima using the B3LYP functional of the density functional theory (DFT), second order Møller-Plesset perturbation theory (MP2) and coupled-cluster with single and double excitations (CCSD) with 6-311++G**, aug-cc-pvdz and aug-cc-pvtz basis sets. The transition state (TS) was requested by a transition state Berry keyword[23], using B3LYP and MP2 methods with 6-311++G** and aug-cc-pvdz basis sets. The Intrinsic Reaction Coordinates (IRCs)[24] were monitored for the transition structures that connect the minima in the potential energy surfaces. The resulting imaginary frequencies and IRCs of the displacements of the bond lengths and angles connecting the atoms of interest were envisaged by GaussView[25] and Chemcraft[26] suites of programs.

The delocalization energies and charge distribution of I, II and transition state were computed by applying Version 3.1 of the Natural Bond Orbital (NBO) program[27] and utilizing B3LYP and MP2 methods with 6-311++G**, aug-cc-pvdz and aug-cc-pvtz basis sets. The NBO donor-acceptor approach was used to explore the relative stabilities of these molecules.

RESULTS AND DISCUSSION

Molecular structure: Fig. 1 depicts the atom numbering of ketenimine (I), acetonitrile (II) and the transition state (TS) together with their optimized bond lengths obtained by using B3LYP/aug-cc-pvdz level of theory. Ketenimine has a Cs point group while acetonitrile (II) has C_{3V} symmetry. As is shown in Table-1, it is apparent that all I and II molecular parameters computed using all the elected levels of theory are comparable. Nonetheless, they seem to show slight dependence on the level of theory used. The MP2 and CCSD methods gave comparable values with longer bond lengths and smaller angles compared to those yielded by the B3LYP functional. The 6-311++G** basis set gave somewhat shorter bond lengths and smaller angles compared to those from aug-cc-pvdz. Our computational resources did not allow us to compute these molecular parameters using the aug-cc-pvtz basis set at the CCSD method to complete the picture; but generally our observations are in good agreement with the results obtained by Watts *et al.*[28]. Rodler *et al.*[29] have derived an experimental value of 115.4 ± 0.6° for HNC angle of ketenimine(I). We managed to reproduce this value to a greater extent using MP2/aug-cc-pvdz (115.52°) and B3LYP/aug-cc-pvdz (115.86°) levels of theory. Our theoretical estimates of the molecular structure of acetonitrile (II) are in excellent agreement with the experimental microwave substitution structure obtained by Kessler *et al.*[30]. The 6-311++G** basis set at all employed levels of theory reproduced the C-H bond lengths almost exactly; while the C-C and CN bond lengths were reproduced to within 0.002Å by B3LYP/aug-cc-pvdz level of theory. The CCSD method with 6-311++G** and aug-cc-pvdz basis sets estimations of the <HCC angles lie within 0.05-0.1° compared to the experimental value[30].

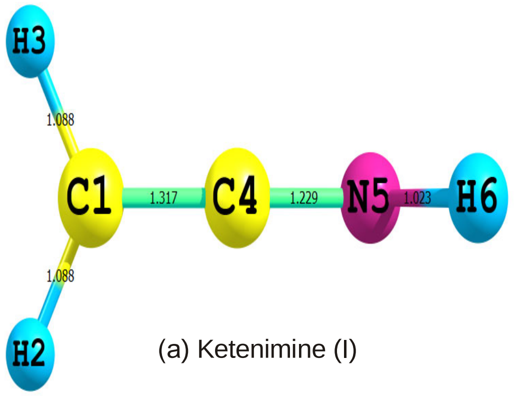

(a) Ketenimine (I)

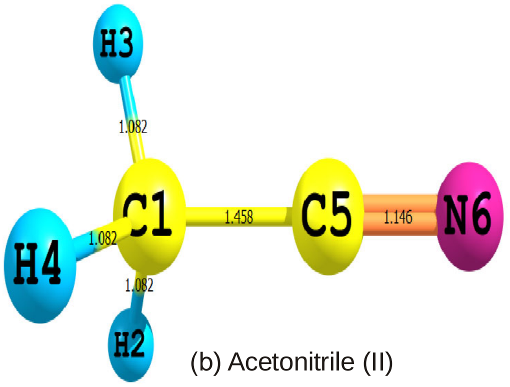

(b) Acetonitrile (II)

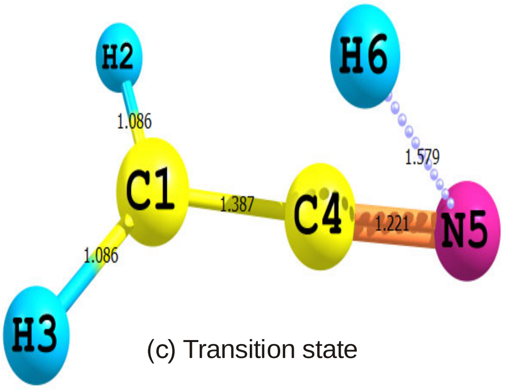

(c) Transition state

Fig. 1. Numbering of atoms for ketenimine (I), the transition state (TS) and acetonitrile (II), together with their optimized bond lengths (Å) obtained using B3LYP/aug-cc-pvdz level of theory

Our B3LYP/aug-cc-pvtz level of theory has estimated the experimental dipole moment of ketenimine[16] of 1.438 Debye to within an error of 0.07%; while the CCSD/aug-cc-pvdz model has reproduced the experimental dipole moment of acetonitrile[31] (3.92 Debye) to within an error of 0.54%.

TABLE-1

OPTIMIZED PARAMETERS [BOND LENGTHS (Å) AND BOND ANGLES (°)] AND DIPOLE MOMENTS (μ/Debye) of $CH_2=C=NH$ (I) AND $CH_3C\equiv N$ (II) USING MP2, B3LYP AND CCSD METHODS WITH 6-311++G** AND aug-cc-pvdz BASIS SETS

Method	Basis Set	C1-H2	N5-H6	C1-C5	CN	<H2C1C5	<C1C5N6	τH3C1C5H2	μ/Debye
MP2	6-311++G**	1.082	1.021	1.319	1.234	120.15	172.95	88.86	1.838
	aug-cc-pvdz	1.090	1.026	1.331	1.244	120.44	173.17	89.24	1.683
	aug-cc-pvtz	1.078	1.018	1.314	1.229	120.44	173.72	89.39	1.639
B3LYP	6-311++G**	1.082	1.020	1.309	1.222	119.19	174.18	89.59	1.594
	aug-cc-pvdz	1.088	1.023	1.317	1.229	119.41	173.68	89.39	1.467
	aug-cc-pvtz	1.080	1.018	1.306	1.219	119.28	174.26	89.52	1.437
CCSD	6-311++G**	1.083	1.021	1.318	1.233	119.89	173.76	89.14	1.670
	aug-cc-pvdz	1.091	1.026	1.330	1.242	120.11	173.98	89.40	1.533
Experimental[a]									1.438
MP2	6-311++G**	1.092	1.092	1.463	1.174	109.89	180.00	120.00	4.301
	aug-cc-pvdz	1.099	1.099	1.471	1.185	109.10	180.00	120.00	4.342
	aug-cc-pvtz	1.087	1.087	1.457	1.169	109.02	180.00	120.00	4.294
B3LYP	6-311++G**	1.092	1.092	1.456	1.153	108.75	180.00	120.00	4.054
	aug-cc-pvdz	1.098	1.098	1.462	1.160	108.89	180.00	120.00	4.054
	aug-cc-pvtz	1.089	1.089	1.456	1.149	108.75	180.00	120.00	4.052
CCSD	6-311++G**	1.093	1.093	1.471	1.160	109.18	180.00	120.00	3.888
	aug-cc-pvdz	1.101	1.101	1.479	1.171	109.23	180.00	120.00	3.941
Experimental[b]		1.092	1.092	1.460	1.158	109.13	180.00	120.00	3.92[c]

[a]Taken from Ref. 16; [b]Taken from Ref. 29. [c]Take from Ref. 30; The first nine lines of data are for I; the second nine lines of data are for II.

Table-2 lists some molecular parameters of I, transition state and II which were computed by using B3LYP/aug-cc-pvdz level of theory. The interconversion between ketenimine (I) and acetonitrile (II) through the transition state (TS), depicted in Fig. 2, can be pursued through the following geometrical parameter changes: (1) Ketenimine CC double bond of 1.317 Å elongated by 0.07 Å in transition state and by another 0.75 Å to form a typical CC single bond in acetonitrile. (2) The CN double bond of 1.229 Å in I was shortened by 0.008 Å in the transition state to settle at 1.160 Å as a typical CN triple bond in II (3) The typical sp^2 HCH angle (about 120°) in both I and transition state was turned into a typical sp^3 angle of 108.89° in II.

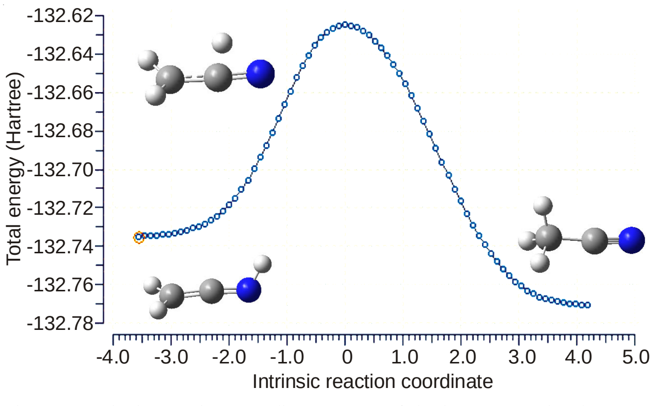

Fig. 2. Intrinsic reaction coordinate (IRC) of the interconversion between ketenimine (I) and acetonitrile (II) through the transition state (TS) which were obtained by using B3LYP/aug-cc-pvdz level of theory

Thermodynamic analysis: Table-3 depicted the ΔE, ΔH, ΔS, ΔG and K values of the tautomerization between ketenimine (I) and acetonitrile (II) which were estimated by using MP2, B3LYP and CCSD methods with 6-311++G**, aug-cc-pvdz and aug-cc-pvtz basis sets. With respect to the modeled levels of theory, the magnitude of these thermodynamic functions follows, more or less, the order MP2 > CCSD > B3LYP for the theoretical methods and 6-311++G** > aug-cc-pvdz > aug-cc-pvtz for the bases sets. It is evident that II is favoured over I and with huge total energy differences ranging from 91.295 to 134.875 kJ/mol at 298.15 K depending on the level of theory used; in excellent agreement with those estimated by Doughty *et al.*[19]. The free energy changes (ΔG) at 298.15 K are extremely dominated by ΔH with little contribution from ΔS. It is noteworthy that the negative values of ΔS denote the preference of II at all temperatures. The K values are sensitive to the values of ΔG *i.e.* a change of about 5 kJ/mol at 298.15 K produces a tenfold value of K. The extremely huge equilibrium concentrations of II compared to those of I at 298.15 K are manifested by the exceedingly large K values. That is, the concentration of II could safely be considered constant at equilibrium. These results are in excellent agreement with experimental and theoretical studies[18,19].

Activation energies: Table-4 enumerated the zero-point electronic and activation energies of the tautomerization of ketenimine (I) and acetonitrile (II) through the transition state (TS) which were estimated by applying MP2, B3LYP and CCSD methods with 6-311++G** and aug-cc-pvdz basis sets. The potential energy profile for this tautomerization using

TABLE-2

SOME OPTIMIZED PARAMETERS [BOND LENGTHS (Å) AND BOND ANGLES (°)] OF KETENIMINE, $CH_2=C=NH$ (I), TRANSITION STATE (TS) AND ACETONITRILE, $CH_3C\equiv N$ (II) WHICH WERE CALCULATED BY USING B3LYP/aug-cc-pvdz LEVEL OF THEORY

Parameter	C-H	C-C	C≡N	NH	<HCH	<CCN	<CNH
I	1.088	1.317	1.229	1.023	119.41	173.68	115.86
TS	1.086	1.387	1.221	1.579	120.93	176.86	47.46
II	1.098	1.462	1.160	–	108.89	180.00	–

TABLE-3
RHF, MP2, B3LYP AND CCSD METHODS AT 6-311++G**, aug-cc-pvdz AND aug-cc-pvtz BASIS SETS
ZERO-POINT REACTION ENERGIES, ENTHALPIES, ENTROPIES, FREE ENERGIES AND
EQUILIBRIUM CONSTANTS FOR EQUILIBRIUM $CH_2=C=NH \rightleftharpoons CH_3C\equiv N$ AT 298.15 K

Method	Basis set	ΔE (kJ/mol)	ΔH (kJ/mol)	ΔS (J/mol K)	ΔG (kJ/mol)	K
RHF	6-311++G**	-129.516	-129.428	-6.946	-127.357	2.057×10^{22}
	aug-cc-pvdz	-125.022	-124.913	-6.846	-122.872	3.369×10^{21}
	aug-cc-pvtz	-124.905	-124.805	-6.862	-122.759	3.218×10^{21}
MP2	6-311++G**	-134.875	-134.926	-7.355	-132.733	1.800×10^{23}
	aug-cc-pvdz	-130.286	-130.260	-6.986	-128.177	2.864×10^{22}
	aug-cc-pvtz	-124.466	-124.445	-6.990	-122.361	2.742×10^{21}
B3LYP	6-311++G**	-95.751	-95.768	-7.342	-93.579	2.483×10^{16}
	aug-cc-pvdz	-91.295	-91.274	-7.114	-89.153	4.167×10^{15}
	aug-cc-pvtz	-92.000	-91.994	-7.258	-89.830	5.475×10^{15}
CCSD	6-311++G**	-126.862	-126.876	-7.325	-124.692	7.020×10^{21}
	aug-cc-pvdz	-121.938	-121.901	-7.060	-119.796	9.741×10^{20}

TABLE-4
ZERO-POINT ELECTRONIC ENERGIES (a.u.) AND ACTIVATION ENERGIES (kcal/mol) OF THE TAUTOMERIZATION OF KETENIMINE ($CH_2=C=NH$) (I) TO FORM ACETONITRILE ($CH_3C\equiv N$) (II) THROUGH TRANSITION STATE (TS) USING HF, B3LYP, MP2 AND CCSD METHODS WITH 6-311++G** AND aug-cc-pvdz BASIS SETS

Method	Basis Set	I	Transition state	II
HF	6-311++G**	-131.865157	-131.733276	-131.914487
	Activ. Energy	82.757	–	113.712
	aug-cc-pvdz	-131.848557	-131.718736	-131.896175
	Activ. Energy	81.464	–	111.345
B3LYP	6-311++G**	-132.714577	-132.609025	-132.751046
	Activ. Energy	66.235	–	89.120
	aug-cc-pvdz	-132.691298	-132.587467	-132.726071
	Activ. Energy	65.155	–	86.975
MP2	6-311++G**	-132.314398	-132.220442	-132.365769
	Activ. Energy	58.958	–	91.194
	aug-cc-pvdz	-132.289043	-132.197902	-132.338666
	Activ. Energy	57.192	–	88.331
CCSD[#]	6-311++G**	-132.3786207	-132.2646727	-132.4286469
	Activ. Energy	71.503	–	102.895
	aug-cc-pvdz	-132.3550435	-132.2441946	-132.40322228
	Activ. Energy	69.559	–	99.791

#single point calculation using B3LYP/aug-cc-pvdz optimized geometry.

B3LYP/aug-cc-pvdz level of theory is depicted in Fig. 2. It is quite obvious that the B3LYP functional has underestimated the energy barriers. The computed activation energies range between 57.066 and 71.489 kcal/mol. Our calculated most accurate value of 69.608 kcal/mol (~0.92 % error) obtained from CCSD/aug-cc-pvtz level of theory is in excellent agreement with the experimental value obtained by Doughty *et al.*[19] of 70.251±0.692 kcal/mol. However, Doughty *et al.*[19] have computed two reaction pathways and energetics for the tautomerization of ketenimine and acetonitrile using MCSCF/DZP level of theory. For both reaction pathways the rate-determining step was the formation of vinyl nitrene through an activation barrier of 75 kcal/mol which is about 5 kcal/mol (~7.1 % error) higher than their experimental value[19]. In the first track, vinyl nitrene rearranged to 2H-azirine that gave acetonitrile through methyl isocyanide. In the second route, vinyl nitrene was reordered directly to acetonitrile through 1,2 H migration. In our calculated route, ketenimine (I) rearranged directly to acetonitrile (II) through 1,3 proton transfer[32,33] and in conformity with allene $\rightleftharpoons$ propyne tautomerization[34].

Based on the above and putting in mind that our CCSD/aug-cc-pvtz activation energy of 69.608 kcal/mol agreed satisfactorily (error < 1%) with the experimental value[19] and that methyl isocyanide has never been detected experimentally in the pyrolysis of vinyl azide[35]; presenting a serious missing link in the 1,2 proton shift pathway proposed by Doughty *et al.*[19]. It is concluded that ketenimine (I) could tautomerize directly to acetonitrile (II) through a 1,3 proton shift, as this pathway proved to be a less energy demanding route. That is why Lohr *et al.*[18] have searched for in the first place, but they were unsuccessful in locating it. We visualized this proton transfer by analyzing the normal mode of the transition state imaginary frequency of -1357.08 cm^{-1}. It is apparent that N5-H6 bond of I has been displaced greatly along the x- and z-axes and thereby the detached proton has been moved from N5 to C1 (Figs. 1 & 3, and Table-4) leading to the formation of acetonitrile (II). We therefore conclude that these mechanistic pathways have established correctly the relationship between the modeled substrates.

Natural bond orbital (NBO) analysis: Fig. 3 depicted the natural atomic charges of I, transition state and II which

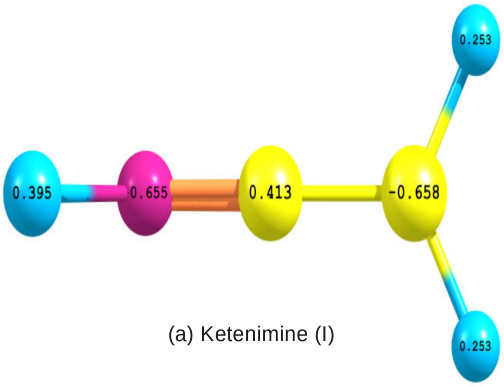

(a) Ketenimine (I)

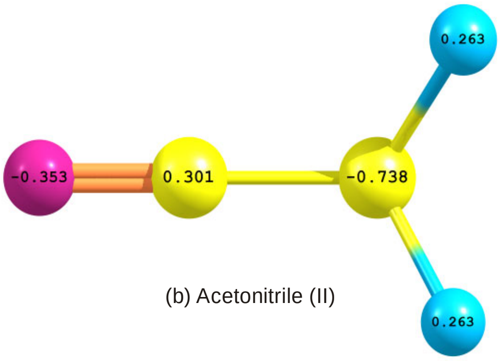

(b) Acetonitrile (II)

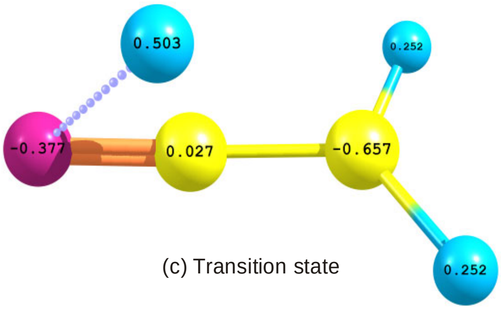

(c) Transition state

Fig. 3. Natural bond orbital charge distribution of (a) ketenimine (I); (b) acetonitrile (IV) and (c) transition state (TS) which were calculated by using B3LYP/aug-cc-pvdz level of theory. The migrating hydrogen atom acquired a positive charge (+0.395e) in I that was intensified (+0.503e) in transition state (TS) and hence migrating to the highly negative (-0.657e) rear carbon atom

were estimated by using B3LYP/aug-cc-pvdz level of theory. The positive charge of I is dispersed amongst the hydrogen atoms (2 × 0.253e and 0.395e) and the middle carbon atom (0.413e). The future leaving H-atom has +0.395e charge. It is apparent that its charge has been intensified (+0.503e) in the transition state and hence being strongly attracted by an intensely negatively charged (-0.657e) rear carbon and not by the positively charged (+0.027e) middle carbon atom to form II. This 1,3 proton migration mechanism actually contradicts that proposed by Doughty *et al.*[19] who computed a 1,2 hydrogen shift using MCSCF/DZP level of theory. In theirs' mechanistic pathway the migrating proton would be attracted by the positively charged middle carbon atom rather than the rear highly negatively charged carbon atom. It is obvious that this is naturally unconceivable.

It is known that the natural bond orbital (NBO) theory[36,37] is quite useful in analyzing hyperconjugative interactions[38] applying second order perturbation energies ($E_{(2)}$):

$$E_{(2)} = \Delta E_{ij} = q_i\,(F_{ij})^2/\Delta\varepsilon$$

where q_i is the donor orbital occupancy, F_{ij} is the off-diagonal elements of the NBO Kohn-Sham Matrix and $\Delta\varepsilon$ is the energy difference between a donor orbital (i) and an acceptor orbital (j). Table-5 lists the second order perturbation ($E_{(2)}$) estimation of the delocalization energies of I, transition state and II which were evaluated by applying B3LYP/aug-cc-pvdz level of theory. It is known that molecules are stabilized/destabilized by three competing factors: electrostatic, steric and hyperconjugative interactions. The energy analysis performed for I, transition state and II in the previous section showed unambiguously that II is by far more stable than I which, in turn, is more stable than the transition state. Putting this fact in mind and having a global look at Table-5 one could come up with the following comments: (1) There is an inverse relation between the overall stability of these substrates and their hyperconjugative energies. That is, the relative stability of II is brought about mostly by acquiring minimal electrostatic and steric interactions; whereas both I and transition state suffer from huge electrostatic repulsions as a result of the proximity of the two double bonds (2) The stabilities of I and, to a greater

TABLE-5
SECOND ORDER PERTURBATION ($E_{(2)}$) ESTIMATION OF THE HYPERCONJUGATIVE ENERGIES (kcal/mol)[a]
OF KETENIMINE $CH_2=C=NH$ (I), TRANSITION STATE (TS) AND ACETONITRILE ($CH_3C\equiv N$) (II)
WHICH WERE CALCULATED USING B3LYP/aug-cc-pvdz LEVEL OF THEORY

Interaction	I	Interaction	Transition state	Interaction	II
$\sigma_{C1-H2}\rightarrow\sigma^*_{C4-N5}$	6.37	$\sigma_{C1-H2}\rightarrow\sigma^*_{C4-N5}$	3.16	$\sigma_{C1-H2}\rightarrow\sigma^*_{C5-N6}$	4.13
$\sigma_{C1-H2}\rightarrow\pi^*_{C4-N5}$	8.65	$\sigma_{C1-H2}\rightarrow\pi^*_{C4-N5}$	3.22	$\sigma_{C1-H2}\rightarrow\pi^*_{C5-N6}$	6.67
$\sigma_{C1-H3}\rightarrow\sigma^*_{C4-N5}$	6.37	$\sigma_{C1-H3}\rightarrow\sigma^*_{C4-N5}$	3.15	$\sigma_{C1-H3}\rightarrow\sigma^*_{C5-N6}$	4.13
$\sigma_{C1-H3}\rightarrow\pi^*_{C4-N5}$	8.65	$\sigma_{C1-H3}\rightarrow\pi^*_{C4-N5}$	3.24	$\sigma_{C1-H3}\rightarrow\pi^*_{C5-N6}$	5.00
$\sigma_{C1-C4}\rightarrow\sigma^*_{C4-N5}$	5.45	$\sigma_{C1-C4}\rightarrow\sigma^*_{C4-N5}$	2.41	$\sigma_{C1-H4}\rightarrow\sigma^*_{C5-N6}$	4.13
$\pi_{C4-C5}\rightarrow\sigma^*_{N5-H6}$	6.62	$\sigma_{C4-H6}\rightarrow\sigma_{C1-N5}$	111.79	$\sigma_{C1-H4}\rightarrow\pi^*_{C5-N6}$	5.00
$\sigma_{C4-N5}\rightarrow\sigma^*_{C1-C4}$	4.76	$\sigma_{C4-N5}\rightarrow\sigma^*_{C1-C4}$	2.78	$\sigma_{C1-C5}\rightarrow\sigma^*_{C5-N6}$	3.92
$\sigma_{N5-H6}\rightarrow\pi^*_{C1-C4}$	16.70	$\sigma^*_{C1-N5}\rightarrow\sigma^*_{C1-C4}$	8.02	$\sigma_{C5-N6}\rightarrow\sigma^*_{C1-C5}$	3.43
$\pi^*_{C1-C4}\rightarrow\sigma^*_{C1-C4}$	8.51	$\sigma^*_{C1-N5}\rightarrow\sigma_{C1-N5}$	2.41	$\pi_{C5-N6}\rightarrow\sigma^*_{C1-H3}$	2.01
$\pi^*_{C1-C4}\rightarrow\sigma^*_{N5-H6}$	2.68	$\sigma^*_{C1-N5}\rightarrow\sigma^*_{C1-N5}$	4.18	$\pi_{C5-N6}\rightarrow\sigma^*_{C1-H4}$	2.01
$n_{N5}\rightarrow\sigma^*_{C1-C4}$	9.86	$n_{N5}\rightarrow\sigma^*_{C1-C4}$	7.07	$\pi_{C5-N6}\rightarrow\sigma^*_{C1-H2}$	2.68
$n_{N5}\rightarrow\pi^*_{C1-C4}$	13.33	$\sigma_{C1-N5}\rightarrow\sigma^*_{C4-H6}$	2.01	$n_{N6}\rightarrow\sigma^*_{C1-C5}$	11.49
Total	97.95	Total	153.44	Total	54.60

[a]Threshold for printing: 0.5 kcal/mol but considered 0.50 kcal/mol when working the totals.

extent, that of transition state, originate mostly from delocalization (3) The most influential hyperconjugative stabilizing interactions of I are the *vicinal*: $\sigma_{N5\text{-}H6}\rightarrow\pi^*_{C1\text{-}C4}$, $n_{N5}\rightarrow\sigma^*_{C1\text{-}C4}$ and $n_{N5}\rightarrow\pi^*_{C1\text{-}C4}$ interactions which contribute 16.70, 9.86 and 13.33 kJ/mol respectively. Nevertheless, the stability of I is hampered by the antibonding *geminal* $\pi^*_{C1\text{-}C4}\rightarrow\sigma^*_{C1\text{-}C4}$ (8.51 kJ/mol) and *vicinal* $\pi^*_{C1\text{-}C4}\rightarrow\sigma^*_{N5\text{-}H6}$ (2.68 kJ/mol) interactions. These antibonding interactions ($\sigma^*_{C1\text{-}N5}\rightarrow\sigma^*_{C1\text{-}C4}$, $\sigma^*_{C1\text{-}N5}\rightarrow\sigma_{C1\text{-}N5}$ and $\sigma^*_{C1\text{-}N5}\rightarrow\sigma^*_{C1\text{-}N5}$) are even more influential in the case of the transition state as they contribute 8.02, 2.41 and 4.18 kJ/mol respectively. As expected they are absent in the most stable tautomer II (4) The transition state extremely strong donor-acceptor coupling between the C4-H6 and C1-N5 σ-bonds of 111.79 kJ/mol is indicative of the comparative weakness of the ketenimine N-H σ-bond and hence its involvement in the 1,3 proton shift to form acetonitrile (5) The most effective delocalization interaction in II is between the N atom lone pair and the C1-C5 σ-bond of 11.49 kJ/mol. This is called the lone pair effect[39].

Conclusion

We used moderately high levels of theory to reinvestigate the mechanistic route of the rearrangement of ketenimine to acetonitrile. Our modeled levels of theory reproduced the experimental geometrical parameters for acetonitrile with excellent precession. The preference of acetonitrile over ketenimine was overwhelmingly reassured by all modeled levels of theory and with total energies ranging between 91.295 to 134.875 kJ/mol at 298.15 K.

Doughty *et al.*[19] experimental and theoretical study of the kinetics of rearrangement of ketenimine to acetonitrile was based on the isoelectronic allene $\rightleftharpoons$ propyne system that assumed inconclusively, in the first place, a 1,2-hydrogen shift rate-determining step.[18,34,40,41] However, there are other studies which postulated a 1,3-proton migration for the tautomerization of allene $\rightleftharpoons$ propyne[35,42]. Our investigation of the ketenimine $\rightleftharpoons$ acetontrile system confirmed the latter and reproduced the experimental activation energy determined by Doughty *et al.*[19] with an error of less than 1 %.

Our proposed 1,3-proton migration rate-determining step route was supported by geometry and electronic charge changes of I, transition state and II as well as by NBO analysis.

ACKNOWLEDGEMENTS

The technological support of King Abdulaziz University through providing the Gaussian Program Version 09 and Chemcraft suites is gratefully acknowledged.

REFERENCES

1. M.S.T. Morin, D.J. St-Cyr, B.A. Arndtsen, E.H. Krenske and K.N. Houk, *J. Am. Chem. Soc.*, **135**, 17349 (2013).
2. E. Zhang, H. Tian, S. Xu, X. Yu and Q. Xu, *Org. Lett.*, **15**, 2704 (2013).
3. M.S.T. Morin, Y. Lu, D.A. Black and B.A. Arndtsen, *J. Org. Chem.*, **77**, 2013 (2012).
4. J.P. Ferris and W.J. Hagan Jr., *Tetrahedron*, **40**, 1093 (1984).
5. E. Herbst, *Angew. Chem. Int. Ed.,* **29**, 595 (1999).
6. R.L. Hudson and M.H. Moore, *Icarus*, **172**, 466 (2004).
7. M.E. Milligan, *J. Chem. Phys.*, **35**, 1491 (1961).
8. D.R. Johnson and F.J. Lovas, *Chem. Phys. Lett.*, **15**, 65 (1972).
9. J.M. Dyke, A.P. Groves, A. Morris, J.S. Ogden, A.A. Dias, A.M.S Oliveira, M.L. Costa, M.T. Barros, M.H. Cabral and A.M.C. Moutinho, *J. Am. Chem. Soc.*, **119**, 6883 (1997).
10. P.D. Godfrey, R.D. Brown, B.J. Robinson and M.W. Sinclair, *Astrophys. J. Lett.*, **13**, 119 (1973).
11. Y.N. Panchenko, S.V. Krasnoshchiokov and C.W. Bock, *J. Comput. Chem.*, **9**, 443 (1988).
12. NguyenSengupta. M.T. Nguyen, D. Sengupta and T.-K. Ha, *J. Phys. Chem.*, **100**, 6499 (1996).
13. J. Zhou and H.B. Schlegel, *J. Phys. Chem. A*, **113**, 9958 (2009).
14. R.D. Brown, E.H.N. Rice and M. Rodler, *Chem. Phys.*, **99**, 347 (1985).
15. M.E. Jacox and D.E. Milligan, *J. Am. Chem. Soc.*, **85**, 278 (1963).
16. M. Rodler, R.D. Brown, P.D. Godfrey and L.M. Tack, *Chem. Phys. Lett.*, **110**, 447 (1984).
17. H.W. Kroto, G.Y. Matti, R.J. Suffolk, J.D. Watts, M. Rittby and R.J. Bartlett, *J. Am. Chem. Soc.*, **112**, 3779 (1990).
18. L.L. Lohr, M. Hanamura and K. Morokuma, *J. Am. Chem. Soc.*, **105**, 5541 (1983).
19. A. Doughty, G.B. Bacskay and J.C. Mackie, *J. Phys. Chem.*, **98**, 13546 (1994).
20. O.I. Osman, Ph.D. Thesis, University of Sussex (1986).
21. O.I. Osman, *J. Phys. Chem. A*, **118**, 10934 (2014).
22. M.J. Frisch, G.W. Trucks, H.B. Schlegel, G.E. Scuseria, M.A. Robb, J.R. Cheeseman, G. Scalmani, V. Barone, B. Mennucci, G.A. Petersson, H. Nakatsuji, M. Caricato, X. Li, H.P. Hratchian, A.F. Izmaylov, J. Bloino, G. Zheng, J.L. Sonnenberg, M. Hada, M. Ehara, K. Toyota, R. Fukuda, J. Hasegawa, M. Ishida, T. Nakajima, Y. Honda, O. Kitao, H. Nakai, T. Vreven, J.A. Montgomery Jr., J.E. Peralta, F. Ogliaro, M. Bearpark, J.J. Heyd, E. Brothers, K.N. Kudin, V.N. Staroverov, R. Kobayashi, J. Normand, K. Raghavachari, A. Rendell, J.C. Burant, S.S. Iyengar, J. Tomasi, M. Cossi, N. Rega, J.M. Millam, M. Klene, J.E. Knox, J.B. Cross, V. Bakken, C. Adamo, J. Jaramillo, R. Gomperts, R.E. Stratmann, O. Yazyev, A.J. Austin, R. Cammi, C. Pomelli, J.W. Ochterski, R.L. Martin, K. Morokuma, V.G. Zakrzewski, G.A. Voth, P. Salvador, J.J. Dannenberg, S. Dapprich, A.D. Daniels, Ö. Farkas, J.B. Foresman, J.V. Ortiz, J. Cioslowski and D.J. Fox, Gaussian 09, Revision A.02, Gaussian, Inc., Wallingford CT (2009).
23. R.S. Berry, P. Davidovits and D.L. McFadden, In Alkali Halide Vapors, Academic Press, New York (1979).
24. K. Fukui, *Acc. Chem. Res.*, **14**, 363 (1981).
25. R. Dennington, T. Keith and J. Millam, GaussView, Version 5; Semichem Inc.: Shawnee Mission, KS, USA (2009).
26. Geomodeling in GeoGraphix, Available online: http://www.chemcraftprog.com (accessed on 26 May 2014).
27. E.A. Reed, L.A. Curtiss and F. Weinhold, *Chem. Rev.*, **88**, 899 (1988).
28. J.D. Watts, D.J. Watts and M.-L. Huang, *J. Phys. Chem. A*, **113**, 1886 (2009).
29. M. Rodler, R.D. Brown, P.D. Godfrey and B. Kleibomer, *J. Mol. Spectrosc.*, **118**, 267 (1986).
30. M. Kessler, H. Ring, R. Trambarulo and W. Gordy, *Phys. Rev.*, **79**, 54 (1950).
31. P.J. Linstrom and W.G. Mallard, eds., NIST Chemistry WebBook, NIST Standard Reference Database Number 69; National Institute of Standards and Technology: Gaithersburg MD; http://webbook.nist.gov (retrieved April 22, 2012).
32. M. Yasumoto, H. Ueki and V.A. Soloshonok, *J. Fluor. Chem.*, **128**, 736 (2007).
33. A. Basak, S.N. Gupta, K. Chakrabarty and G.K. Das, *Compt. Theor. Chem.*, **1007**, 15 (2013).
34. T. Kakumoto, T. Ushirogouchi, K. Saito and A. Imamura, *J. Phys. Chem.*, **91**, 183 (1987).
35. A. Lifshitz, M. Frenklach and A. Burcat, *J. Phys. Chem.*, **79**, 1148 (1975).
36. E.A. Reed, L.A. Curtiss and F. Weinhold, *Chem. Rev.*, **88**, 899 (1988).
37. E.A. Reed and F. Weinhold, *J. Chem. Phys.*, **78**, 4066 (1983).
38. L. Song, Y. Lin, W. Wu, Q. Zhang and Y. Mo, *J. Phys. Chem. A*, **109**, 2310 (2005).
39. T. Yamamoto, D. Kaneno and D. Tomoda, *Bull. Chem. Soc. Jpn.*, **81**, 1415 (2008).
40. M. Yoshimine, J. Pacansky and N. Honjou, *J. Am. Chem. Soc.*, **111**, 4198 (1989).
41. C. Wentrup, C.M. Nunes and I. Reva, *J. Phys. Chem. A*, **118**, 5122 (2014).
42. J.N. Bradley and K.O. West, *J. Chem. Soc., Faraday Trans. I*, **71**, 967 (1975).